

## MIL03346, the most oxidized Martian meteorite: A first look at spectroscopy, petrography, and mineral chemistry

M. Darby Dyar,<sup>1</sup> Allan H. Treiman,<sup>2</sup> Carlé M. Pieters,<sup>3</sup> Takahiro Hiroi,<sup>3</sup> Melissa D. Lane,<sup>4</sup> and Vanessa O'Connor<sup>5</sup>

Received 5 March 2005; revised 14 May 2005; accepted 6 June 2005; published 15 September 2005.

[1] Meteorite MIL03346, recovered from Antarctica, is a nakhlite: an augite clinopyroxenite inferred to have originated from Mars' surface. MIL03346 contains ~70% augite and 3% olivine in a fine-grained mesostasis of basaltic glass, olivine, titanomagnetite, and pyrrhotite. Part of the olivine is altered to fine-grained ferric clays and oxides: "iddingsite" as described in other nakhlites. Chemical compositions of augite and olivine (FeO/MnO and Fe/Mg) are nearly identical to those of other nakhlites and are consistent with a Martian origin. The augite contains significant Fe<sup>3+</sup>: ~24% of total iron by Mössbauer spectroscopy and ~13% by elemental analyses and crystal chemistry. This proportion of Fe<sup>3+</sup> in augite is consistent with high-temperature equilibration near the QFM oxygen buffer. Thermal emission spectra are similar to those of other nakhlites. Visible to mid-IR spectra of MIL03346 show the same absorption features as do other nakhlites but at distinctly lower reflectances (which likely represent Fe<sup>3+</sup> in augite and magnetite). MIL03346 appears to contain the most Fe<sup>3+</sup> of any Martian meteorite studied to date and to have come from the most oxidizing magmatic environment yet reported.

**Citation:** Dyar, M. D., A. H. Treiman, C. M. Pieters, T. Hiroi, M. D. Lane, and V. O'Connor (2005), MIL03346, the most oxidized Martian meteorite: A first look at spectroscopy, petrography, and mineral chemistry, *J. Geophys. Res.*, *110*, E09005, doi:10.1029/2005JE002426.

### 1. Introduction

[2] The Martian (SNC) meteorites are critically important for understanding Mars because they provide details of petrography and chemistry that cannot (yet) be measured in situ, and they provide "ground truths" for spectral analyses from the Martian surface using Mössbauer, thermal emission, and visible, near-IR, and mid-IR reflectance techniques. The recent discovery of a new 815 g Martian meteorite in the Miller Range of Antarctica [Satterwhite and Richter, 2004] provides us with a new sample with which to test hypotheses developed in studies of other nakhlite samples. Here we present results of an integrated series of measurements made on MIL03346 in order to relate them to other SNCs and to expand our understanding of Martian geology.

### 2. Background

[3] More than 30 meteorites from Mars are now known, all basalts or fractionates from basaltic magma. The Martian

origin of these samples is confirmed by their isotopic and chemical compositions as compared to the few similar in situ analyses at Mars [Treiman *et al.*, 2000].

[4] Among Martian meteorites the seven known nakhlites (including MIL03346) are a closely related group of augite-rich cumulate igneous rocks that formed in flows or shallow intrusions of basaltic magmas [Treiman, 2005]. The most abundant mineral in the nakhlites is subcalcite augite; the nakhlites also contain lesser and variable proportions of olivine, low-calcium pyroxene ( $\pm$ pigeonite  $\pm$  orthopyroxene), plagioclase, Fe-Ti oxides, pyrrhotite, other minor minerals, and the alteration material iddingsite (a reddish submicron mixture of smectite, iron oxy-hydroxides, and salts). Iddingsite is formed by alteration of olivine or basalt glass by liquid water. In most nakhlites it is clear that the iddingsite was formed on Mars.

### 3. Methods

[5] Polished thin sections (.6 and .93) and a 528 mg whole rock sample of MIL03346 (.49) were allocated to the authors. From the latter a 100 mg chip was set aside for thermal emission spectroscopy, and ~100 mg was ground and sieved to <45  $\mu$ m and >45  $\mu$ m size fractions for both reflectance and emission spectroscopic study. Splits of those powders were used for Mössbauer spectrometry. The remaining 328 mg were gently crushed by hand at Mount Holyoke. Clinopyroxene grains were handpicked from the sample; special care was taken to avoid incorporation of grains with reddish rinds that suggest alteration. Again,

<sup>1</sup>Department of Astronomy, Mount Holyoke College, South Hadley, Massachusetts, USA.

<sup>2</sup>Lunar and Planetary Institute, Houston, Texas, USA.

<sup>3</sup>Department of Geological Sciences, Brown University, Providence, Rhode Island, USA.

<sup>4</sup>Planetary Science Institute, Tucson, Arizona, USA.

<sup>5</sup>Department of Geology, Smith College, Northampton, Massachusetts, USA.

**Table 1.** Mineral Chemical Compositions and Cation Proportions

	MIL03346			Nakhla Augite Core	NWA817 Augite Core	Lafayette Augite Core	Y000593 Augite Core
	Olivine Core <sup>a</sup>	Augite Rim	Augite Core				
SiO <sub>2</sub>	33.84	43.25	51.39	52.62	51.93	51.79	52.66
TiO <sub>2</sub>	0.02	2.09	0.26	0.12	0.30	0.28	0.11
Al <sub>2</sub> O <sub>3</sub>	0.02	7.70	0.86	0.53	0.94	0.93	0.50
Cr <sub>2</sub> O <sub>3</sub>	0.01	0.00	0.32	0.39	0.46	0.47	0.41
FeO	46.02	25.52	13.73	14.06	13.48	13.80	14.39
MnO	0.94	0.59	0.42	0.44	0.39	0.42	0.44
MgO	19.03	2.16	13.00	13.57	13.13	13.60	13.38
CaO	0.56	19.30	19.53	18.58	19.74	18.97	18.62
Na <sub>2</sub> O	0.01	0.42	0.28	0.19	0.32	0.22	0.18
K <sub>2</sub> O	0.00	0.00	0.00	0.00	0.00	0.00	0.01
Oxide total	100.46	99.26	99.79	100.51	100.69	100.48	100.69
Ca	0.018	0.842	0.790	0.749	0.794	0.764	0.750
Mg	0.833	0.131	0.732	0.761	0.734	0.762	0.750
Fe <sup>2+</sup>	1.120	0.769	0.329	0.431	0.369	0.384	0.443
Fe <sup>3+</sup>	0.010	0.100	0.104	0.011	0.054	0.050	0.010
Mn	0.023	0.020	0.013	0.014	0.013	0.013	0.014
Cr	0.000	0.000	0.010	0.012	0.015	0.015	0.013
Na	0.000	0.033	0.021	0.014	0.024	0.016	0.013
Al <sup>VI</sup>	0.000	0.105	0.000	0.007	0.000	0.006	0.000
Al <sup>IV</sup>	0.001	0.177	0.038	0.024	0.041	0.041	0.022
Ti	0.001	0.064	0.007	0.003	0.008	0.008	0.003
Si	0.994	1.760	1.941	1.980	1.948	1.947	1.981
Fe <sup>3+</sup> calc, <sup>b</sup> %	1	12	14	2	13	12	2
Fe <sup>3+</sup> Möss, <sup>c</sup> %	NA	24	24	2	NA	NA	NA

<sup>a</sup>Olivine core is average core olivine, normalized to 3 cations and +8 charge. Augite core is average core augite, normalized to 4 cations and +12 charge; augite rim is a single spot analysis. NA is not analyzed.

<sup>b</sup>Percent Fe<sup>3+</sup>calc is calculated as described in the text.

<sup>c</sup>Percent Fe<sup>3+</sup>Möss is from this work and *Dyar* [2003]; note that these values represent bulk analyses.

two splits were created: one for thermal IR reflectance and emission analyses and one for Mössbauer analyses. Sample masses for visible/IR measurements ranged from 5 to 34 mg. In all cases, reflectance and emission measurements used exactly the same samples.

[6] Petrographic descriptions are from optical and scanning electron microscope/backscatter electron studies of thin sections. Mineral chemical analyses (Table 1) were obtained by electron microprobe with the Cameca SX100 in the Astromaterials Research and Exploration Science (ARES) division, Johnson Space Center. In addition to MIL03346, SNCs Lafayette, Nakhla, NWA817, and Y000593 were also analyzed in order to have a set of comparable analyses acquired with the same standards in the same sessions. Analytical conditions were 15 kV accelerating potential, beam current of 20 nA, and count times 20–30 s on peak. Analytical standards were spessartine for Mn, chromium metal for Cr, and Kakanui kaersutite for the other elements.

[7] X-ray diffraction (XRD) of a whole rock sample was done at Smith College on their Scintag SDX-2000 diffractometer. A step size of 0.020°, a scan rate of 0.10° min<sup>-1</sup>, and 12 s count times were used over a range of 5.00°–70.00° 2θ. A Cu Kα tube with a wavelength of 1.540562 Å was used.

[8] Visible to near-infrared bidirectional reflectance spectra (0.3–2.6 μm, 5 nm sampling resolution) were acquired relative to halon at 30° incident and 0° emergent angles using the Reflectance Experiment Laboratory (RELAB) bidirectional spectrometer. The same samples (in the same dish) were measured using a Pike diffuse reflectance attachment (off-axis and biconical) with the Thermo Nexus

870 Fourier transform infrared (FTIR) spectrometer (2–50 μm) located at the RELAB, using a diffuse gold standard. The data were typically spliced at 2.5 μm to use the absolute reflectance of the bidirectional system. Detailed descriptions of the RELAB facility instruments are given by *Pieters and Hiroi* [2004] and are available at <http://www.planetary.brown.edu/rehab/>.

[9] Mössbauer spectra were acquired at room temperature as well as 16 K to determine Fe<sup>2+</sup> and Fe<sup>3+</sup> mineral species. A source of 45 mCi <sup>57</sup>Co in Rh was used on a WEB Research Co. model W100 spectrometer. Run times ranged from 1 to 2 days. Results were calibrated against an α-Fe foil of 6 μm thickness and 99% purity. Data were fit using the methods and software described by *Eeckhout and DeGrave* [2003d].

[10] Emissivity spectra (2000–250 cm<sup>-1</sup>) were obtained at Arizona State University using a modified Nicolet FTIR spectrometer equipped with a CsI beam splitter and an uncooled deuterated triglycine sulfate detector. The system atmosphere is scrubbed using a Parker Balston compressed air and gas in-line filter, and the sample chamber is kept at a constant temperature (~24.7°C). The samples were maintained at ~80°C using a sample-cup heater, and the spectra were acquired over 270 scans at 2 cm<sup>-1</sup> sampling. Details of the instrument calibration and data reduction strategy are given by *Ruff et al.* [1997].

## 4. Results

### 4.1. Petrography

[11] MIL03346 is a naxhlite (Figure 1a) [*Treiman*, 2005] with 70.8% augite and 3.0% olivine crystals (including

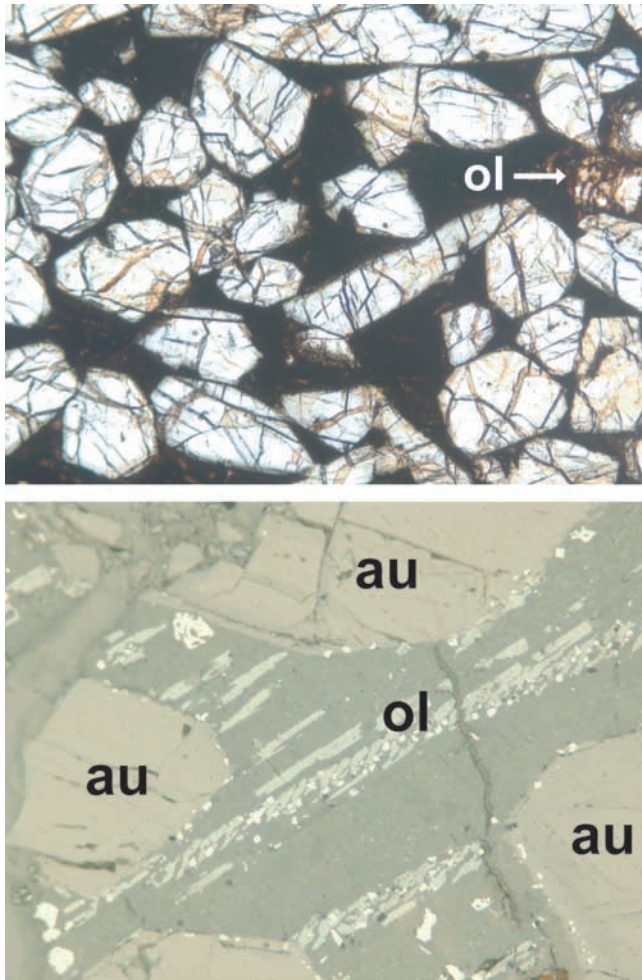


**Figure 1.** Thin sectional views of MIL03346. (top) General textures, plane polarized light, 2.3 mm across. Clear, slightly greenish augite crystals and an olivine grain (ol) in dark, fine-grained mesostasis are shown. The olivine is cut by veinlets of hydrous alteration material (iddingsite), and cracks across augite contain films of ferric "rust." (bottom) Mesostasis texture, plane-reflected light, 0.58 mm across. Large equant grains are augite (au); mesostasis among them is basaltic glass olivine as long "spinifex" olivine crystals (ol) and titanomagnetite in skeletal shapes and as tiny grains (lightest shade).

~0.2% iddingsite) in fine-grained mesostasis (optical count of 1428 points). Molar Fe/Mn ratios of 33 in augite and 50 in olivine (Table 1) are consistent with a Martian origin [Papike *et al.*, 2003; Satterwhite and Righter, 2004]. Augite crystals in MIL03346 are euhedral prisms, to 1.5 mm long and 0.2–0.3 mm across, with typical octagonal cross sections. Most augite grains have a chemically homogeneous core,  $Wo_{40}En_{37}$  (Table 1), with rare inclusions of glass and altered glass. Surrounding each core is a rim, to ~30  $\mu\text{m}$  thick, of increasing to extreme enrichment in Fe, Al, and Ti (Table 1). In some areas, augite crystals show lamellar twins and granulation indicating rapid deformation. No pigeonite or orthopyroxene was observed.

[12] Large olivine grains in MIL03346 are subhedral to  $2 \times 1$  mm and are euhedral where they abut mesostasis and

irregular where they abut augite. Their cores are homogeneous ( $Fo_{43}$ ), with rounded augite inclusions and magmatic inclusions of pyroxene dendrites in silicate glass. Surrounding the core is a rim, to ~50  $\mu\text{m}$  thick, of increasing enrichment in Fe. Among these large augite and olivine crystals is mesostasis, consisting of dendritic skeletal crystals of olivine and titanomagnetite in silicate glass (Figure 1b), small ellipsoidal grains of pyrrhotite (possibly immiscible sulfide melt), and rare lilac-colored "fassaite" (high-Ti-Al augite). The titanomagnetite contains fine exsolution lamellae of ilmenite.

[13] Olivine in MIL03346 has been partially altered to fine-grained, reddish-brown material like the iddingsite in other nakhlites [Gooding *et al.*, 1991; Gillet *et al.*, 2002]. It typically occurs as veinlets cutting olivine, with yellow-orange birefringent material (smectite?) in the cores and reddish irregular grains (ferric oxy-hydroxide?) at the rims. At least some of the iddingsite is terrestrial, as it occurs undeformed among twinned and granulated augite grains.

#### 4.2. Electron Microprobe Analysis

[14] Mineral analyses (Table 1) produce results that are typical for nakhlite augite and olivine [Treiman, 2005]. For the augite analyses to fulfill pyroxene stoichiometry (4 cations with a total charge of +12 to charge balance 6 oxygens), approximately 10% of their iron must be  $Fe^{3+}$ . The need for  $Fe^{3+}$  is not a simple analytical artifact, because olivine analyzed at the same time normalizes properly with minimal  $Fe^{3+}$  (3 cations summing to +8 charge). Of the other nakhlite augites analyzed with the same instrument and conditions within 2 months of each other for this study, NWA817 and Lafayette also required ~10%  $Fe^{3+}$  for proper normalization, while Nakhla and Y000593 required nearly none.

#### 4.3. X-Ray Diffraction

[15] XRD results showed the presence of 16% olivine and 84% pyroxene. No other phases were detected. These abundances are consistent with the presence of abundant olivine (and perhaps some fine-grained pyroxene) in the mesostasis, as noted in section 4.1 and by Hammer and Rutherford [2005].

#### 4.4. Mössbauer

[16] Mössbauer spectra of whole rock and clinopyroxene separates of MIL03346 are shown in Figure 2. The Mössbauer doublets fit to the spectra are described in terms of two parameters for such paramagnetic minerals: (1) Isomer shift ( $\delta$ ), which is sometimes called center shift, arises from the difference in *s*-electron density between the nuclei of the radioactive source and that at the absorbing iron nuclei in the sample. (2) Quadrupole splitting arises from an electric field gradient at the nucleus, which produces two (or more, in the case of magnetic materials) energy levels when nuclear charge distributions are nonspherical (as they are in the majority of minerals). Quadrupole splitting is defined as the separation between the two component peaks of a doublet, and isomer shift is the difference between the midpoint of the doublet and zero on the velocity scale. On the basis of hundreds of analyses of minerals with known Fe valence states and site occupancies, it is observed that  $Fe^{2+}$  doublets have significantly larger  $\delta$  and  $\Delta$  values than  $Fe^{3+}$

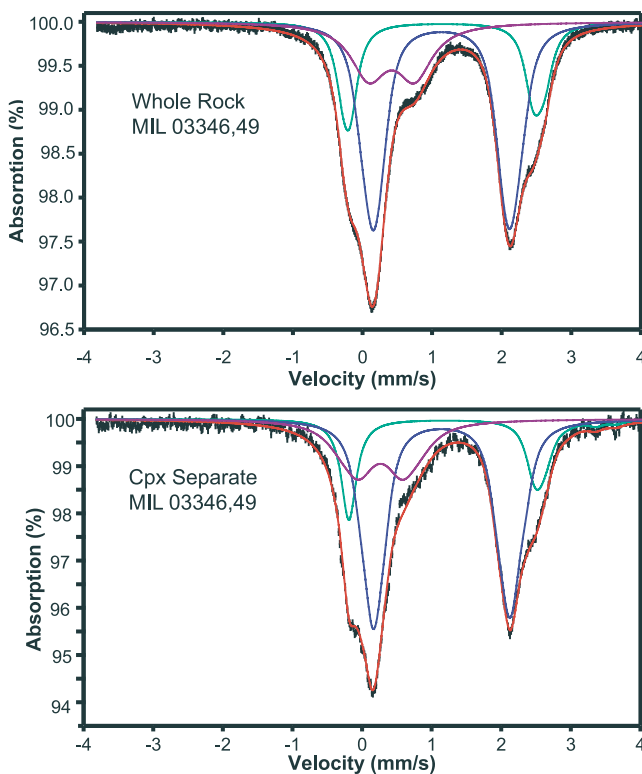


**Figure 2.** Mössbauer spectra of (top) whole rock and (bottom) clinopyroxene (cpx) separates from MIL03346,49. Green and blue doublets represent  $\text{Fe}^{2+}$  in clinopyroxene while the purple curve represents  $\text{Fe}^{3+}$ . Olivine peaks would lie at  $-0.36$  and  $2.64 \text{ mm s}^{-1}$  and could not be resolved in either of these spectra, but a small amount of olivine could be present and masked because of the peak overlap with pyroxene. The orange curve represents the sum of all the component curves. Magnetite, if present, would have a prominent peak at  $-3.6 \text{ mm s}^{-1}$ . There may be a hint of that peak in both spectra, but it is well below the 1% detection limit.

[Burns and Solberg, 1990]. Similarly, clinopyroxene and olivine have different parameters because the coordination polyhedra in these two minerals are quite different (i.e., chain silicates versus orthosilicates). Clinopyroxene  $\text{Fe}^{2+}$  doublets commonly have parameters of  $\delta = 1.14\text{--}1.18 \text{ mm s}^{-1}$  and  $\Delta = \sim 2.30\text{--}2.74$  and  $\sim 2.00 \text{ mm s}^{-1}$  (two different doublets) at room temperature [e.g., Dyar et al., 1989; Dyar, 2003; Eeckhout and DeGrave, 2003a, 2003b, 2003c]; many other silicates, including nearly all the other chain and sheet silicates (pyroxenes, amphiboles, micas, chlorites, etc.) have very similar Mössbauer parameters for  $\text{Fe}^{2+}$  in octahedral coordination. Olivine, on the other hand, has what are, for silicates, rather unusual parameters of roughly  $\delta = 1.10\text{--}1.16 \text{ mm s}^{-1}$  and  $\Delta = 2.80\text{--}3.20 \text{ mm s}^{-1}$  [e.g., Dyar et al., 1989]. Because the olivine peaks lie on the outermost shoulders of most silicate rock spectra, they are relatively easy to resolve and may be considered diagnostic of olivine if only silicates are present in the rock. The presence of magnetic phases (hematite, magnetite, etc.) is also easily recognized because their Mössbauer spectra consist of sextets due to magnetic splitting of nuclear energy levels.

[17] Both MIL03346 spectra show typical features for clinopyroxene (Table 2), consistent with parameters observed in the other SNCs previously studied [Dyar, 2003]. These include isomer shift values of  $1.14\text{--}1.16 \text{ mm s}^{-1}$  and quadrupole splitting values of  $2.60\text{--}2.68 \text{ mm s}^{-1}$  for one  $\text{Fe}^{2+}$  doublet and  $1.95\text{--}1.97 \text{ mm s}^{-1}$  for the other. The area of these bands is roughly proportional to the percentage of the total Fe that is present as  $\text{Fe}^{2+}$  in clinopyroxenes, though recoil-free fraction effects may introduce a minor adjustment to those peak areas (see Eeckhout and DeGrave [2003a, 2003b, 2003c] for more information).

[18] Neither spectrum shows any clear signs of olivine, which would show up as a conspicuous doublet (at energies of roughly  $-0.36$  and  $2.64 \text{ mm s}^{-1}$ ) on the outer shoulders of the pyroxene features (the outermost of which lie at  $-0.12$  and  $2.48 \text{ mm s}^{-1}$ ) because of its broad quadrupole splitting as noted above. Olivine is distributed irregularly (e.g., the thin section examined by Satterwhite and Righter [2004] had none), and the chip from which our splits for spectroscopic analysis were made (49) may have had little olivine. An olivine doublet would have been expected from the abundance of olivine ( $\sim 3\%$ ) and the iron content ( $\text{Fa}_{57}$ ) of the whole meteorite; furthermore, the other spectroscopic techniques in this study observed small amounts of olivine in splits from the same samples. We attempted to refit these spectra with an olivine component, but such a doublet could not be uniquely resolved. Therefore we can only rule out the presence of olivine above about a 3% level because the peaks would overlap with those of pyroxene. Given the other spectroscopic evidence presented here, olivine may well be present in roughly that amount.

[19] The Mössbauer spectra show no evidence for the presence of magnetite within the detection limits of the technique for nonoverlapping peaks (0.5–1% of the total Fe). A typical magnetite spectrum consists of a complicated superposition of sextets from Fe in different sites; for the present paper, it is sufficient to note that a prominent magnetite peak appears at an energy of  $\sim -3.6 \text{ mm s}^{-1}$  [e.g., Schwertman and Murad, 1990]. However, a slight inflection in the baseline of the whole rock spectrum at  $-3.75 \text{ mm s}^{-1}$  suggests its possible presence at levels of

**Table 2.** Mössbauer Parameters for MIL03346,49<sup>a</sup>

	Whole Rock	Clinopyroxene
$\text{Fe}^{2+}$		
QS	2.60	2.68
CS	1.14	1.15
Width	0.26	0.26
Area	23.1	19.8
$\text{Fe}^{2+}$		
QS	1.95	1.97
CS	1.13	1.15
Width	0.26	0.26
Area	54.2	56.1
$\text{Fe}^{3+}$		
QS	0.66	0.61
IS	0.42	0.27
Width	0.62	0.55
Area	22.8	24.2
$\chi^2$	1.33	5.67

<sup>a</sup>QS is quadrupole splitting. CS is center shift. IS is isomer shift. All parameters are given in  $\text{mm s}^{-1}$ .

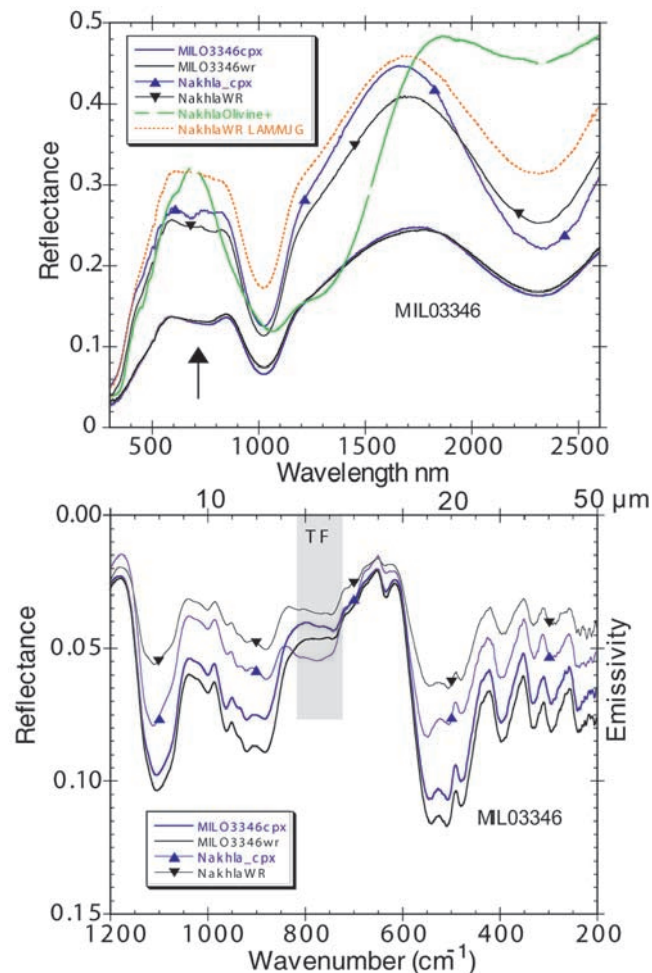


**Figure 3.** Reflectance spectra of MIL03346,49 whole rock (wr) and cpx separates and similar Nakhla samples. (top) Bidirectional visible near-IR reflectance. Arrow indicates  $\text{Fe}^{2+}$ – $\text{Fe}^{3+}$  intervalence charge transfer feature. (bottom) Mid-IR reflectance. Except for the transparency feature (TF), which is dependent on particle size, almost all features can be attributed to high-Ca clinopyroxene [Hamilton, 2000].

<1% of the total Fe. Thus  $\text{Fe}^{3+}$  in magnetite is unlikely to contribute to the significant  $\text{Fe}^{3+}$  doublets observed in both spectra.

[20] Both the whole rock and the clinopyroxene separate were also run at 16 K in the hopes of increasing peak separation and perhaps causing magnetic splitting in phases other than pyroxene that are overlapped at room temperature. Although the doublets showed the expected shifts as a function of the low temperature, the fit results proved identical to those at room temperature. The low-temperature spectra were dominated by pyroxene doublets, and no resolvable magnetic peaks (or anything resembling an alteration phase) appeared.

[21] The similarity of all the spectra reflects both the modal distribution of phases and their relative Fe contents. Because the Mössbauer technique “sees” only Fe atoms, the doublet areas of Fe-richer phases may be considerably exaggerated relative to their true modal abundances, so any

magnetite (72 wt % Fe) would be more easily detected relative to the augite (10–19 wt % Fe). Even if Fe in magnetite made up a full 1% of the total Fe by percentage, its corresponding modal abundance would only be roughly 0.1%. The difference between the augite separate and the bulk sample is the addition of mesostasis in the latter, but the similarity in the two spectra suggests that most of the iron is in pyroxene or a phase with similar Mössbauer parameters (perhaps olivine or glass). The presence of magnetite at >0.5% of the mode would be readily apparent in the Mössbauer spectra, and it is simply not observed.

[22] These MIL03346 spectra are unique among the SNCs in that they both show a significant proportion of the total iron as  $\text{Fe}^{3+}$  (23% and 24% for whole rock and clinopyroxene (cpx) separate, respectively). Previously, the most oxidized SNC was ALHA 84001 at 4.5%  $\text{Fe}^{3+}$  [Dyar, 2003]. Unfortunately, many phases have the same parameters for  $\text{Fe}^{3+}$ , so the mineralogy of the  $\text{Fe}^{3+}$ -bearing phase cannot be determined from the Mössbauer spectra alone. This raises the question of the mineral host for the  $\text{Fe}^{3+}$ , which cannot be either olivine or magnetite by the reasoning just presented. The only possibility other than augite is that  $\text{Fe}^{3+}$  might be contained in the iddingsite. Alteration veinlets in the olivine were measured by electron microprobe and are roughly 37.5 wt % FeO (29 wt %  $\text{Fe}^{2+}$  or 26.3 wt %  $\text{Fe}^{3+}$ ). However, their modal abundance is estimated at roughly 0.1%. Thus even if the alteration was pure  $\text{Fe}^{3+}$ , it would still not constitute a significant enough proportion of the total Fe in the sample to be detected at the 1% level.

#### 4.5. Visible, Near-IR, and Mid-IR Reflectance Spectra

[23] Reflectance spectra are shown in Figure 3. Spectra of the MIL03346 whole rock and cpx separates are shown along with whole rock and mineral separates of Nakhla prepared in a similar manner by our spectroscopy consortium [Pieters et al., 2004; Sunshine et al., 2004]. As with the Mössbauer results the spectrum of MIL03346 clinopyroxene separate is almost identical to the parent whole rock spectrum. All MIL03346 features observed are due to features of high-Ca pyroxene (with the exception of the transparency feature near  $800\text{ cm}^{-1}$ ). In addition to the bands at 1 and  $2.3\ \mu\text{m}$  due to  $\text{Fe}^{2+}$  in the M2 pyroxene site and a band at  $1.2\ \mu\text{m}$  due to  $\text{Fe}^{2+}$  in the M1 site [e.g., Burns, 1993], MIL03346 contains a prominent feature in the visible region near  $0.7$ – $0.8\ \mu\text{m}$ . Although visible wavelength absorptions in pyroxene are commonly attributed to Cr, the MIL03346 augite contains little Cr (Table 1), and the absorption occurs at a distinctly lower energy than electronic transitions of Cr. Given the significant abundance of  $\text{Fe}^{3+}$  in the MIL03346 augite, the assignment of this feature is most consistent with  $\text{Fe}$ – $\text{Fe}^{3+}$  intervalence charge transfer (IVCT) transitions [Burns, 1993]. Note that IVCT transitions occur too rapidly to be evident in Mössbauer spectra and do not affect the quantification of  $\text{Fe}^{3+}$  by that technique.

[24] Recognizing the potential importance of the  $\text{Fe}^{2+}$ – $\text{Fe}^{3+}$  IVCT feature at visible wavelengths for remote sensing analyses, we have included an independent whole rock spectrum of the Nakhla meteorite (data courtesy of L. A. McFadden and M. J. Gaffey) for comparison [McFadden and Cline, 2005]. As with our consortium spectra of Nakhla whole rock a  $\text{Fe}^{2+}$ – $\text{Fe}^{3+}$  feature is not evident (but may be

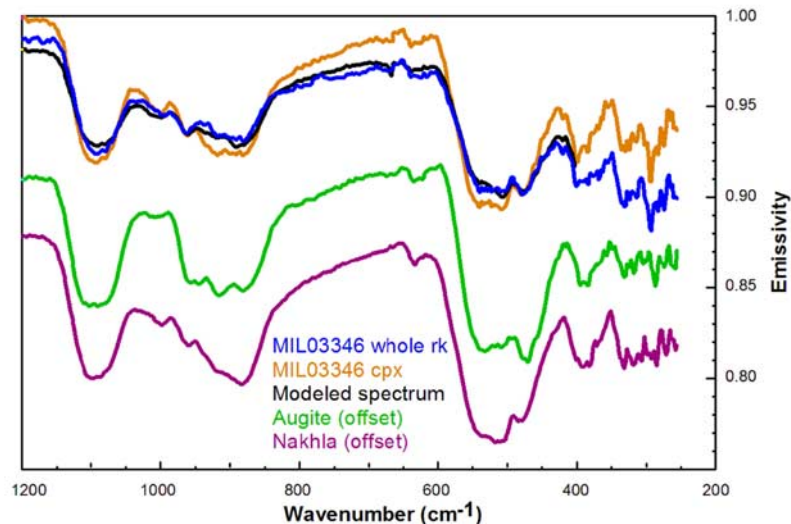


**Figure 4.** Thermal emission spectra of MIL03346,49 whole rock and cpx separates, a modeled whole rock spectrum, an offset augite spectrum (BUR-620) from the Arizona State University spectral library [Christensen *et al.*, 2000], and an offset Nakhla spectrum [Hamilton *et al.*, 2003] (different sample from that of Figure 3) for comparison.

masked by an olivine peak in the same part of the spectrum). Although the pyroxene of MIL03346 is very similar to that of Nakhla, there are some important differences between the two meteorites. To a first order the  $\text{Fe}^{2+}$  bands of MIL03346 in the near IR are comparable to those of Nakhla, but the MIL03346 spectra are distinctly darker (corroborating the visual observations). This albedo difference could be affected by particle size differences between the two samples, but it is most likely due to an inherent property of the MIL03346 samples, such as their more oxidized composition and the presence of the absorbing mesostasis.

[25] Broad differences between the spectral features of MIL03346 and Nakhla are linked to their bulk mineralogy, namely, that MIL03346 is nearly monomineralic (clinopyroxene) and that Nakhla contains small, but significant, amounts of Fe-rich olivine. The presence of olivine in Nakhla reduces the relative strength of the  $2.3\ \mu\text{m}$  band in the whole rock spectrum. A peak in Nakhla olivine reflectance in the visible would also reduce any  $0.7\ \mu\text{m}$  feature present in the whole rock spectra. Because neither Nakhla nor MIL03346 exhibits OH features in the near infrared, there is no evidence of clay in either. Differences between these samples of the two meteorites are more subtle in the mid infrared. Although these mid-infrared reflectance spectra have not been explicitly modeled with potential end-members, the features observed are all consistent with those of high-Ca pyroxene [Hamilton, 2000].

#### 4.6. Thermal Emission Spectra

[26] Emissivity spectra of the MIL03346 whole rock chip and the pyroxene separate are shown in Figure 4 along with an offset spectrum of augite [Christensen *et al.*, 2000]. It is clear by visual comparison of the augite spectrum with the meteorite spectra that the meteorite is dominated by clinopyroxene. This result was confirmed through spectral deconvolution [e.g., Ramsey and Christensen, 1998] using

an end-member suite of rock-forming minerals that included the augite separate from the MIL03346 meteorite itself. The modeled meteorite spectrum retrieved from the deconvolution is shown in Figure 4. The spectral deconvolutions of the whole rock returned predominantly augite (at 81.2%), a value that approximates (but overestimates) the augites that were point counted in the optical petrographic data and is very close to the XRD estimate of augite content.

[27] Minor amounts of other minerals, at or below confident detection limits, were selected in the deconvolution for fine-tuning of the spectral fits (including enstatite, an orthopyroxene that is not actually in the meteorite, at  $\sim 5\%$ , the highest percentage of the “other” minerals). Both basaltic and silicic glass were end-members as were both forsteritic and fayalitic olivine; however, neither glass nor olivine was identified in the deconvolution.

[28] The emissivity spectrum of MIL03346 is very similar to the emissivity spectrum of Nakhla (another augite-dominated meteorite) from Hamilton *et al.* [2003] (Figure 4). However, Nakhla contains slightly more olivine (5–18% [Friedman Lentz *et al.*, 1999] versus  $\sim 3\%$  in MIL03346) and additional plagioclase feldspar. The deeper bands at  $\sim 515$  and  $\sim 885\ \text{cm}^{-1}$  in the Nakhla spectrum likely are due to the greater amount of olivine present in the sample.

#### 5. Most Oxidized Martian Rock?

[29] Multiple lines of evidence from this study point to an oxidized source region for MIL03346 rather than postcrystallization alteration. The Mössbauer data constrain the amount of  $\text{Fe}^{3+}$  present to be 23–24% of the total Fe atoms. Electron microprobe analysis (EMPA) data suggest a need for roughly 10%  $\text{Fe}^{3+}$  to maintain charge balance in the augite; considering the propagated errors on this calculation, the value agrees with the Mössbauer results (the EMPA calculations are at best qualitative but at least provide an

**Table 3.** Modal Calculations for Distribution of Fe Atoms<sup>a</sup>

Phase	Present, %	Modal, %	Fe Atoms, per Formula Unit	Z/Unit Cell Volume	Fe Atoms per Unit Cell of Phase	Fe Atoms per 1000 Å of Rock	Fe Atoms in Phase, %
Large crystals							
Forsterite (olivine)		2.8	1.12	4/290	15.45	0.43	5.7
Augite (pyroxene)		70.8	0.87	4/447	7.77	5.50	72.5
Iddingsite		0.2	2.05	4/290	28.28	0.06	0.7
Mesostasis phases							
Silica	4	1.0	0.00	3/113	0.00	0.00	0.0
Glass	69	18.1	0.39	4/450	3.47	0.63	8.3
Titanomagnetite	4	1.0	3.00	8/591	40.62	0.43	5.6
Phosphate	3	0.8	0.00	2/528	0.00	0.00	0.0
Fayalite (olivine)	8	2.1	1.12	4/290	15.45	0.32	4.3
Augite (pyroxene)	11	2.9	0.87	4/447	7.77	0.22	3.0

<sup>a</sup>Unit cell information is from <http://www.webmineral.com>. Mesostasis modes courtesy of J. Hammer. All other data are from this study.

estimate of the need to consider the possible presence of Fe<sup>3+</sup> or not).

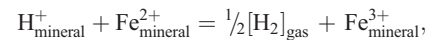
[30] A relatively simple calculation can be done to demonstrate why the Fe<sup>3+</sup> observed in the Mössbauer spectra must be largely in the augite crystals (Table 3) rather than in other phases. The calculation needs to make two assumptions. (1) The mesostasis mode must be approximated; for this purpose we have used data generously provided by J. Hammer (personal communication, 2005): 4% silica, 69% glass, 4% titanomagnetite, 11% pyroxene, 3% phosphate, and 8% fayalite. (2) Volumes for the iddingsite and glass must be assumed; here we use values similar to olivine and pyroxene. The calculation simply takes the number of Fe atoms in each unit cell and calculates how many Fe atoms would be present in a unit volume of the rock, using the modes. The result (far right column in Table 3) shows that 85.5% of the Fe atoms in this rock must be in either olivine or pyroxene. If all the remaining Fe in the glass was completely oxidized (extremely unlikely), then, including the Fe<sup>3+</sup> in the titanomagnetite, only ~14% of the Fe in the rock would be Fe<sup>3+</sup> in those phases, leaving ~10% of the total Fe that would have to be in pyroxene and olivine. More realistically, the glass + titanomagnetite might be 30–50% Fe<sup>3+</sup>, which would result in ~17% of the total Fe atoms being Fe<sup>3+</sup> in olivine or pyroxene. Because olivine rarely accommodates Fe<sup>3+</sup> in its crystal structure, by far the most likely location for the Fe<sup>3+</sup> is in the augite.

[31] This calculation is relatively independent of the actual modes represented in the mesostasis. The point is that the majority of the Fe atoms in the bulk rock are in pyroxene and olivine, so with the large amount of Fe<sup>3+</sup> observed by the Mössbauer measurement, there are just not that many places for the Fe<sup>3+</sup> to go. Therefore we conclude that the Fe<sup>3+</sup> contents quantified by Mössbauer spectroscopy represent Fe<sup>3+</sup> in the augite itself.

[32] Although this much Fe<sup>3+</sup> is large relative to the other SNC meteorites studies using Mössbauer [Dyar, 2003], it is, in fact, typical of terrestrial mantle and magmatic pyroxenes that equilibrated at the relatively oxidizing conditions of the QFM oxygen buffer [Dyar *et al.*, 1989, 1992; Ionov and Wood, 1992; Luth and Canil, 1993; McCanta *et al.*, 2004]. It is possible that this level of oxidation is not uncommon in nakhlites. As shown in Table 1, the NWA817 and Lafayette meteorites also have significant calculated Fe<sup>3+</sup> in augite (NWA998 also has a

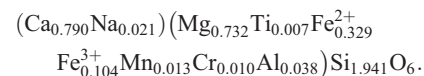
calculated Fe<sup>3+</sup> content of 17% based on data given by Treiman [2005]). Aliquots of sufficient size for handpicking of a Mössbauer quantity clinopyroxene separate are unavailable for these meteorites.

[33] It must be noted that the presence of Fe<sup>3+</sup> in pyroxene is not always an indication of an oxidizing source region but may instead reflect a hydrous source region. The mechanism for this process is dehydrogenation, in which the charge on the H protons is left behind as polarons on Fe atoms. The reaction by which this loss of hydrogen occurs may be



as described by Mackwell and Kohlstedt [1990] for olivine and Skogby [1994] for synthetic magnesian clinopyroxene. In other words, hydrogen loss may result in a concomitant increase in Fe<sup>3+</sup> concentration, resulting in H contents and Fe<sup>3+</sup>/Fe<sup>2+</sup> ratios that are significantly out of equilibrium with the oxygen (and hydrogen) fugacity before dehydrogenation occurred. In the present study, we must consider the possibility that MIL03346 was vulnerable to loss of hydrogen during shock, excavation, and transport.

[34] To test the possible effects of this hypothesis, we first assume that the before-impact composition of the sample was a completely Fe<sup>2+</sup> augite with a composition that can be represented by our average core analysis (Table 1):



[35] We then ask the question: What weight percent H<sub>2</sub>O would give rise to a formula with all Fe<sup>2+</sup> and the 0.104 per formula unit H? An iterative calculation can be done to answer this question, which results in a formula of (Ca<sub>0.790</sub>Na<sub>0.021</sub>)(Mg<sub>0.732</sub>Ti<sub>0.007</sub>Fe<sub>0.434</sub><sup>2+</sup>Mn<sub>0.013</sub>Cr<sub>0.010</sub>Al<sub>0.038</sub>)Si<sub>1.941</sub>O<sub>6</sub> and a calculated 0.41 wt % H<sub>2</sub>O. Work on the solubility of H in pyroxene by Bell *et al.* [1995] and Bell and Rossman [1992] suggests that mantle clinopyroxene may contain up to 0.04 wt % H<sub>2</sub>O, while the as-erupted H<sub>2</sub>O content of mantle clinopyroxene is 0.0184 wt %. These amounts are significantly smaller than the 0.41 wt % H<sub>2</sub>O calculated. It is therefore likely that only a very small proportion of the Fe<sup>3+</sup> in MIL03346 could be due to dehydrogenation. Thus our results suggest that the

Martian source region of this meteorite was indeed significantly more oxidizing than those for the other SNCs.

[36] The oxygen fugacity ( $f_{O_2}$ ) of Martian basalts has previously been estimated using several means. *Wadhwa* [2001] used Eu/Gd partitioning in augite to show a difference in SNC redox state of more than 3 log units, ranging from QFM-1.6 down to QFM-5, but she did not analyze any of the nakhlites. *Herd et al.* [2001] studied many of the same meteorites using titanomagnetite stoichiometry to calculate oxygen fugacity; he reports a range from QFM-3.0 to QFM-1.0 ( $\pm 0.5$  log units). They also recognized that subsolidus reequilibration of the oxides could have occurred. So *Herd et al.* [2002a] showed a correlation between  $D_{Eu}/D_{Gd}$  (where  $D$  is the distribution coefficient) and  $f_{O_2}$  derived from oxides, with an offset of 1–2 log units. While further work is in progress to reconcile these two methods for measuring  $f_{O_2}$ , a third method based on the equilibrium  $6FeSiO_3 + 2Fe_2O_3 = 6Fe_2SiO_4 + O_2$  [cf. *Wood*, 1991] is reported by *Herd et al.* [2002b] and *Herd* [2003] that gives a range of  $f_{O_2}$  from QFM-3.7 to QFM + 0.2 (the latter value represents estimates made from late crystallizing Ol-Px-Sp groups). It is important to note that these studies focused largely on shergottite meteorites. Isotope systematics [e.g., *Borg et al.*, 2003] have suggested that metasomatism have caused systematic difference between the shergottites, which have been extensively studied, and the nakhlites and Chassigny, which have not.

[37] However, a few other studies provide data on the oxidation states of the nakhlites. *Szymanski et al.* [2003, 2004] used Fe-Ti oxides to study Nakhla, Lafayette, Y000593, and NWA998 and reported  $f_{O_2}$  values of QFM + 0.1  $\pm$  0.6. *Chevrier and Lorand* [2005] reported that sulfide mineralogy in nakhlites is consistent with magmatic redox conditions at roughly QFM, while experimental evidence from *Hammer and Rutherford* [2005] supports crystallization of MIL03346 in a “moderately oxidizing environment.”

[38] In order to estimate  $f_{O_2}$  on the basis of our spectroscopic results we use a fourth method based on the relationship between  $Fe^{3+}$  in Ca-rich pyroxene and  $f_{O_2}$  as determined experimentally [*McCanta et al.*, 2004]. This calibration is only useful at high values of  $f_{O_2}$  ( $> \approx$ QFM) and so is not useful for most shergottite basalts. The most oxidized pyroxene in the McCanta et al. study was in equilibrium with QFM + 0.5 because that study was focused on the  $f_{O_2}$  believed at that time to be analogous to Martian conditions. However, if their calibration curve is extended to more oxidizing conditions (in fact, work is in progress to perform those experiments), our results on MIL03346 pyroxene suggest an  $f_{O_2}$  of  $\sim$ QFM + 1.5. These contrast with the other shergottite and chassignite pyroxenes studied by *Dyar* [2003], which had so little  $Fe^{3+}$  that they could not be used to estimate crystallization oxygen fugacity.

[39] The  $Fe^{2+}$ – $Fe^{3+}$  IVCT feature present in MIL03346 spectra may prove to be an important tool for remote mineral analysis of the Martian surface because the abundance of  $Fe^{3+}$  in pyroxene is linked to key magmatic processes and degree of oxidation in the geologic history of Mars. Among the SNCs analyzed, this feature appears to be unique to MIL03346 [e.g., *McFadden and Cline*, 2005; *Pieters et al.*, 2004]. Detection of the  $Fe^{2+}$ – $Fe^{3+}$  IVCT feature in the visible spectrum will be challenging, however, and will likely require the high spatial and spectral resolu-

tion of instruments like Observatoire pour la Minéralogie, l’Eau, les Glaces et l’Activité (OMEGA) and Compact Reconnaissance Imaging Spectrometer for Mars (CRISM).

[40] **Acknowledgments.** M.D.L. thanks P. Christensen for the generous use of his spectrometer facility. We thank John Brady for his assistance with the XRD measurement, Julia Hammer for the new data on modes in the mesostasis, and Vicky Hamilton for the Nakhla emission spectrum. Support for this work from NASA grants NNG04GB53G, NNG04GG12G, NAG5-12687, NAG5-12271, and NAG5-13279 is gratefully acknowledged. RELAB is a multiuser facility operated under NASA grant NAG5-13609. This is Lunar and Planetary Institute contribution 1238. We thank Vicky Hamilton, Phil Bland, and an anonymous reviewer for thoughtful reviews of this manuscript, which greatly improved it.

## References

- Bell, D. R., and G. R. Rossman (1992), Water in Earth’s mantle: The role of nominally anhydrous minerals, *Science*, 255, 1391–1397.
- Bell, D. R., P. D. Ihinger, and G. R. Rossman (1995), Quantitative analysis of trace OH in garnet and pyroxenes, *Am. Mineral.*, 80, 465–474.
- Borg, L. E., L. E. Nyquist, H. Weismann, C. Y. Shih, and Y. Reese (2003), The age of Dar al Gani 476 and the differentiation history of the Martian meteorites inferred from their radiogenic isotopic systematics, *Geochim. Cosmochim. Acta*, 67, 3519–3536.
- Burns, R. G. (1993), *Mineralogical Applications of Crystal Field Theory*, 2nd ed., 551 pp., Cambridge Univ. Press, New York.
- Burns, R. G., and T. C. Solberg (1990), Spectroscopic characterization of minerals and their surfaces, *ACS Symp. Ser.*, 415, 262–283.
- Chevrier, V., and J. P. Lorand (2005), Sulfide mineralogy, redox conditions, and alteration effects in some SNC meteorites, *Lunar Planet. Sci. [CD-ROM]*, XXXVII, Abstract 2067.
- Christensen, P. R., J. L. Bandfield, V. E. Hamilton, D. A. Howard, M. D. Lane, J. L. Piatek, S. W. Ruff, and W. L. Stefanov (2000), A thermal emission spectral library of rock-forming minerals, *J. Geophys. Res.*, 105, 9735–9739.
- Dyar, M. D. (2003), Ferric iron in SNC meteorites as determined by Mössbauer spectroscopy: Implications for Martian landers and Martian oxygen fugacity, *Meteorit. Planet. Sci.*, 38, 1733–1752.
- Dyar, M. D., A. V. McGuire, and R. D. Ziegler (1989), Redox equilibria and crystal chemistry of coexisting minerals from spinel lherzolite mantle xenoliths, *Am. Mineral.*, 74, 969–980.
- Dyar, M. D., A. V. McGuire, and M. D. Harrell (1992), Crystal chemistry of iron in contrasting styles of metasomatism in the upper mantle, *Geochim. Cosmochim. Acta*, 56, 2579–2586.
- Eeckhout, S. G., and E. DeGrave (2003a),  $^{57}Fe$  Mössbauer-effect studies of Ca-rich, Fe-bearing clinopyroxenes: Part I. Paramagnetic spectra of magnesian hedenbergite, *Am. Mineral.*, 88, 1129–1137.
- Eeckhout, S. G., and E. DeGrave (2003b),  $^{57}Fe$  Mössbauer effects studies of Ca-rich, Fe-bearing clinopyroxenes: Part II. Magnetic spectra of magnesian hedenbergite, *Am. Mineral.*, 88, 1138–1144.
- Eeckhout, S. G., and E. DeGrave (2003c),  $^{57}Fe$  Mössbauer effects studies of Ca-rich, Fe-bearing clinopyroxenes: Part III. Diopside, *Am. Mineral.*, 88, 1145–1152.
- Eeckhout, S. G., and E. DeGrave (2003d), Evaluation of ferrous and ferric Mössbauer fractions. part II, *Phys. Chem. Miner.*, 30, 142–146.
- Friedman Lentz, R. C., G. J. Taylor, and A. H. Treiman (1999), Formation of a Martian pyroxenite: A comparative study of the nakhlite meteorites and Theo’s flow, *Meteorit. Planet. Sci.*, 34, 919–932.
- Gillet, P., J. A. Barrat, E. Deloule, M. Wadhwa, A. Jambon, V. Sautter, B. Devouard, D. Neuville, K. Benzerara, and M. Lesourd (2002), Aqueous alteration in the northwest Africa 817 (NWA 817) Martian meteorite, *Earth Planet. Sci. Lett.*, 203, 431–444.
- Gooding, J. L., S. J. Wentworth, and M. E. Zolensky (1991), Aqueous alteration of the Nakhla meteorite, *Meteorit. Planet. Sci.*, 26, 135–143.
- Hamilton, V. E. (2000), Thermal infrared emission spectroscopy of the pyroxene mineral series, *J. Geophys. Res.*, 105, 9701–9716.
- Hamilton, V. E., P. R. Christensen, H. Y. McSween Jr., and J. L. Bandfield (2003), Searching for the source regions of Martian meteorites using MGS TES: Integrating Martian meteorites into the global distribution of igneous materials on Mars, *Meteorit. Planet. Sci.*, 38, 871–885.
- Hammer, J. E., and M. J. Rutherford (2005), Experimental crystallization of Fe-rich basalt: Application to cooling rate and oxygen fugacity of nakhlite MIL 03346, *Lunar Planet. Sci. [CD-ROM]*, XXXVI, Abstract 1999.
- Herd, C. D. K. (2003), The oxygen fugacity of olivine-phyric Martian basalts and the components within the mantle and crust of Mars, *Meteorit. Planet. Sci.*, 38, 1793–1805.

- Herd, C. D. K., J. J. Papike, and A. J. Brearley (2001), Oxygen fugacity of Martian basalts from electron microprobe oxygen and TEM-EELS analyses of Fe-Ti oxides, *Am. Mineral.*, *86*, 1015–1024.
- Herd, C. D. K., L. E. Borg, J. H. Jones, and J. J. Papike (2002a), Oxygen fugacity and geochemical variations in the Martian basalts: Implications for Martian basalt petrogenesis and the oxidation state of the upper mantle, *Geochim. Cosmochim. Acta*, *66*, 2025–2036.
- Herd, C. D. K., C. S. Schwandt, J. H. Jones, and J. J. Papike (2002b), An experimental and petrography investigation of Elephant Moraine 79001 lithology A: Implications for its petrogenesis and the partitioning of chromium and vanadium in a Martian basalt, *Meteorit. Planet. Sci.*, *37*, 987–1000.
- Ionov, D. A., and B. J. Wood (1992), The oxidation state of subcontinental mantle: Oxygen thermobarometry of mantle xenoliths from central Asia, *Contrib. Mineral. Petrol.*, *111*, 179–193.
- Luth, R. W., and D. Canil (1993), Ferric iron in mantle-derived pyroxenes and a new oxybarometer for the mantle, *Contrib. Mineral. Petrol.*, *113*, 236–248.
- Mackwell, S. J., and D. L. Kohlstedt (1990), Diffusion of hydrogen in olivine: Implications for water in the mantle, *J. Geophys. Res.*, *95*, 5079–5088.
- McCanta, M. C., M. D. Dyar, M. J. Rutherford, and J. S. Delaney (2004), Iron partitioning between basalt and clinopyroxene as a function of oxygen fugacity, *Am. Mineral.*, *89*, 1685–1693.
- McFadden, L. A., and T. P. Cline (2005), Spectral reflectance of Martian meteorites: Spectral signatures as a template for locating source region on Mars, *Meteorit. Planet. Sci.*, *40*, 151–172.
- Papike, J. J., J. M. Karner, and C. K. Shearer (2003), Determination of planetary basalt parentage: A simple technique using the electron microprobe, *Am. Mineral.*, *88*, 469–472.
- Pieters, C. M., and T. Hiroi (2004), RELAB (Reflectance Experiment Laboratory): A NASA multiuser spectroscopy facility, *Lunar Planet. Sci.* [CD-ROM], XXXV, Abstract 1720.
- Pieters, C. M., M. D. Dyar, T. Hiroi, J. Bishop, J. Sunshine, and R. Klima (2004), Pigeonite masquerading as olivine at Mars: First results from the Mars Spectroscopy Consortium, *Lunar Planet. Sci.* [CD-ROM], XXXV, Abstract 1171.
- Ramsey, M. S., and P. R. Christensen (1998), Mineral abundance determination: Quantitative deconvolution of thermal emission spectra, *J. Geophys. Res.*, *103*, 577–596.
- Ruff, S. W., P. R. Christensen, and P. W. Barbera (1997), Quantitative thermal emission spectroscopy of minerals: A laboratory technique for measurement and calibration, *J. Geophys. Res.*, *102*, 14,899–14,913.
- Satterwhite, C., and K. Righter (2004), Special Edition: Announcing the availability of a new Martian meteorite, *Antarct. Meteorit. Newsl.*, *27*(2), 1–2.
- Schwertman, U., and E. Murad (1990), The influence of aluminum on iron oxides: Al-substituted magnetite synthesized at ambient temperatures, *Clays Clay Miner.*, *38*, 196–202.
- Skogby, H. (1994), OH incorporation in synthetic clinopyroxene, *Am. Mineral.*, *79*, 240–249.
- Sunshine, J. M., J. Bishop, M. D. Dyar, T. Hiroi, R. Klima, and C. M. Pieters (2004), Near-infrared spectra of Martian pyroxene separates: First results from the Mars Spectroscopy Consortium, *Lunar Planet. Sci.* [CD-ROM], XXXV, Abstract 1636.
- Szymanski, A., F. E. Brenker, A. El Goresy, and H. Palme (2003), Complex thermal history of nakhlite and Y000593, *Lunar Planet. Sci.* [CD-ROM], XXXVI, Abstract 1922.
- Szymanski, A., F. E. Brenker, H. Palme, and A. El Goresy (2004), Thermobarometry of Martian nakhlites and a lherzolite—A comparison, paper presented at 67th Meeting, Meteorit. Soc., Houston, Tex.
- Treiman, A. H. (2005), The nakhlite Martian meteorites: Augite-rich igneous rock from Mars, *Chem. Erde*, *65*, in press.
- Treiman, A. H., J. D. Gleason, and D. D. Bogard (2000), The SNC meteorites are from Mars, *Planet. Space Sci.*, *48*, 1213–1230.
- Wadhwa, M. (2001), Redox state of Mars' upper mantle and crust from Eu anomalies in shergottite pyroxenes, *Science*, *291*, 1527–1530.
- Wood, B. J. (1991), Oxygen barometry of spinel peridotites, in *Oxide Minerals: Petrologic and Magnetic Significance*, edited by D. H. Lindsley, *Rev. Mineral.*, *14*, 417–431.
- M. D. Dyar, Department of Astronomy, Mount Holyoke College, 50 College St., Kendade Hall, Room 217, South Hadley, MA 01075, USA. (mdyar@mtholyoke.edu)
- T. Hiroi and C. M. Pieters, Department of Geological Sciences, Brown University, Providence, RI 02912, USA.
- M. D. Lane, Planetary Science Institute, 1700 E. Fort Lowell Rd., Suite 106, Tucson, AZ 85719, USA.
- V. O'Connor, Department of Geology, Smith College, Northampton, MA 01063, USA.
- A. H. Treiman, Lunar and Planetary Institute, 3600 Bay Area Blvd., Houston, TX 77058, USA.